Nano Research 2018, 11(2): 905–912
https://doi.org/10.1007/s12274-017-1701-5
Research Article
ISSN 1998-0124
CN 11-5974/O4

50 ppm of Pd dispersed on $Ni(OH)_2$ nanosheets catalyzing semi-hydrogenation of acetylene with high activity and selectivity

Mingzhen Hu[1], Jian Zhang[2], Wei Zhu[2], Zheng Chen[2], Xin Gao[2], Xianjun Du[2], Jiawei Wan[2], Kebin Zhou[1] (✉), Chen Chen[2] (✉), and Yadong Li[2]

[1] *School of Chemistry and Chemical Engineering, University of Chinese Academy of Sciences, Beijing 100049, China*
[2] *Department of Chemistry, Tsinghua University, Beijing 100084, China*

Received: 13 March 2017
Revised: 6 June 2017
Accepted: 8 June 2017

KEYWORDS
catalyst,
trace-loading,
palladium,
hydrogenation

ABSTRACT

We report a highly efficient $Pd/Ni(OH)_2$ catalyst loaded with ultra-low levels of palladium (50 ppm Pd by mass) for the selective hydrogenation of acetylene to ethylene. The turnover frequency for acetylene conversion over the 0.005% $Pd/Ni(OH)_2$ catalyst is twice that of the equivalent 0.8% $Pd/Ni(OH)_2$ catalyst. Notably, an acetylene-to-ethylene selectivity of 80% was achieved over a wide range of temperatures. Aberration-corrected high-angle annular dark-field scanning transmission electron microscopy was used to reveal the atomically dispersed nature of palladium in the 0.005% $Pd/Ni(OH)_2$ catalyst. The excellent selectivity of this catalyst is attributed to its atomically dispersed Pd sites, while the abundant hydroxyl groups of the support significantly enhance the acetylene conversion activity. This work opens up innovative opportunities for new types of highly efficient catalysts with trace noble-metal loadings for a wide variety of reactions.

1 Introduction

Raw ethylene produced by cracking commonly contains about 1% coproduced acetylene, which must be removed or reduced to an acceptable level to avoid downstream catalyst poisoning and the degradation of polyethylene quality during ethylene polymerization [1, 2]. Selective hydrogenation over an effective catalyst is the most widely employed strategy for removing trace acetylene in raw ethylene. After extensive screening of a variety of metals, palladium is recognized to be the state-of-the-art catalyst for the selective hydrogenation of acetylene, but its high cost and poor selectivity toward ethylene inevitably limits its utilization [3]. Intense research effort has been directed toward the development of highly selective and cost-effective catalysts with low levels of palladium, or that are palladium-free, for this reaction [4, 5].

Address correspondence to Kebin Zhou, kbzhou@ucas.ac.cn; Chen Chen, cchen@mail.tsinghua.edu.cn

Through density functional theory (DFT) calculations and experimental exploration, Nørskov and co-workers demonstrated that nickel-zinc alloys serve as promising alternatives to Pd for the hydrogenation of acetylene, with superior ethylene selectivity [6]. Our group has also developed a series of intermetallic Ni_xM_y catalysts that display excellent selectivities for the formation of ethylene [7]. However, alternative non-palladium catalysts usually require relatively high reaction temperatures that fall short of industrial requirements. Alloying Pd with a second metal modifier to form bimetallic catalysts has proven to be another effective approach for decreasing Pd content and improving the corresponding ethylene selectivity by rationally tuning the electronic or geometric structures of Pd [8–11]. However, these palladium-based alloy catalysts often require complex preparation procedures and retain considerable palladium content, which greatly increases their preparation and production costs. For example, commercial Pd-Pb/$CaCO_3$ catalysts are generally loaded with more than 1% Pd, and even the most effective Pd-Ag alloy catalyst is loaded with about 0.1% Pd [12, 13].

Recently, single-atom or atomically dispersed metal catalysts, with fully exposed active sites, have aroused significant interest in the field of heterogeneous catalysis, due to their high atom efficiencies, reduced costs, and their prospects for industrial upscaling [14–18]. In addition, compared with traditional metal nanoparticle catalysts, they sometimes exhibit intriguing activities and selectivities [19]. In this communication, we describe the preparation of an atomically dispersed and ultra-low-loaded Pd catalyst (50 ppm by mass) supported on $Ni(OH)_2$ nanosheets; the prepared 0.005% Pd/$Ni(OH)_2$ catalyst exhibits excellent catalytic activity and selectivity for the hydrogenation of acetylene, as illustrated in Fig. 1.

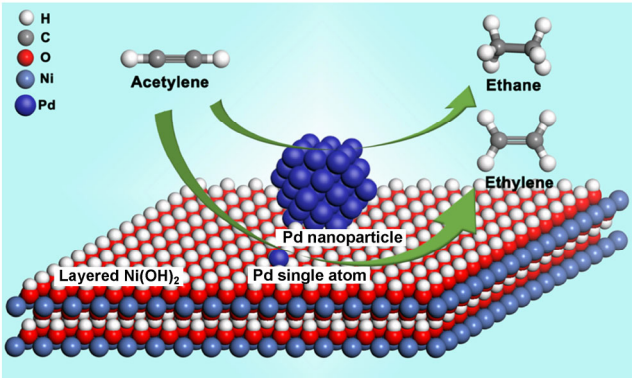

Figure 1 Schematic illustration of atomically dispersed and nanosized Pd supported on $Ni(OH)_2$ nanosheets for the selective catalytic hydrogenation of acetylene.

2 Experimental section

2.1 Materials

Nickel(II) nitrate hexahydrate and urea were purchased from Tianjin Jinke Fine Chemical Institute. Potassium borohydride and triethylene glycol were purchased from Sinopharm Chemical Reagent Beijing Co., Ltd. Sodium tetrachloropalladate(II) was purchased from Sigma-Aldrich. All chemicals were of analytical grade and used as received, without further purification. The water used in all experiments was purified through a Millipore system.

2.2 Preparation of the $Ni(OH)_2$ support

The $Ni(OH)_2$ support was prepared according to the method reported by Du et al. [20]. In a typical synthesis, nickel(II) nitrate hexahydrate (1.45 g) was dissolved in a water/triethylene glycol mixed solvent system. Urea was then added under mild stirring to obtain a homogeneous solution. The entire solution was transferred to a Teflon-lined stainless-steel autoclave, sealed and maintained at 120 ˚C for 24 h. After cooling to room temperature, the resulting precipitate was isolated by centrifugation, and washed several times with ethanol and pure water. Finally, the product was dried overnight in air at 60 ˚C.

2.3 Preparation of the 0.005% Pd/$Ni(OH)_2$ catalyst

The 0.005% Pd/$Ni(OH)_2$ catalyst was prepared as follows. First, the appropriate amount of sodium tetrachloropalladate(II) solution was added to a well-dispersed $Ni(OH)_2$ suspension to obtain the required Pd loading. The suspension was vigorously stirred for 24 h to form a solid surface combination of the positively charged $Ni(OH)_2$ support and the negatively charged tetrachloropalladate(II) anions. The precursor was centrifuged and washed several times with pure water and dried overnight under vacuum at 40 ˚C.

Finally, the obtained precursor was reduced with hydrogen at 160 ℃.

2.4 Preparation of the 0.8% Pd/Ni(OH)$_2$ catalyst

The 0.8% Pd/Ni(OH)$_2$ catalyst was prepared using a similar method to that described in section 2.3 (above). First, the appropriate amount of sodium tetrachloropalladate(II) solution was added to a well-dispersed Ni(OH)$_2$ suspension. The suspension was vigorously stirred for 24 h to obtain a solid combination of the Ni(OH)$_2$ support and the tetrachloropalladate(II) anions. The precursor was centrifuged, washed several times with pure water and dried overnight under vacuum at 40 ℃. Finally, the obtained precursor was reduced with a potassium borohydride solution (0.1 g·L^{-1}), centrifuged, washed several times with pure water and dried overnight under vacuum at 40 ℃.

2.5 Preparation of the 0.005% Pd/NiO catalyst

The 0.005% Pd/NiO catalyst was prepared by calcination of the 0.005% Pd/Ni(OH)$_2$ catalyst at 300 ℃ for two hours under argon.

2.6 Preparation of the 0.005% Pd/SiO$_2$-*T* catalyst

A mesoporous SiO$_2$ support was prepared according to a published procedure [21]. The mesoporous SiO$_2$ support was dispersed in pure water and homogenized by sonication. The appropriate amount of sodium tetrachloropalladate(II) solution was added to the above suspension to obtain the required nominal Pd loading, vigorously stirred for 24 h, centrifuged, washed several times with pure water and dried overnight under vacuum at 40 ℃. The obtained precursor was then calcined at either 300 or 750 ℃. The 0.005% Pd/SiO$_2$-*T* catalyst products were finally obtained by reduction of the above calcined precursors with hydrogen at 160 ℃.

2.7 Preparation of the 0.005% Pd/SiO$_2$-750RD catalyst

The 0.005% Pd/SiO$_2$-750RD catalyst was prepared in a similar manner to that described in section 2.6 (above), except that after calcination at 750 ℃ the 0.005% Pd/SiO$_2$-750RD precursor was re-dispersed in water for 24 h to restore the OH content of the support.

2.8 Characterization

The crystallographic structures of the products were determined by powder X-ray diffraction (XRD, Bruker D8 Focus X-ray diffractometer, Cu Kα radiation, λ = 0.1542 nm). Transmission electron microscopy (TEM) was carried out on a Jeol JEM-2100F FETEM instrument. High angle annular dark field scanning TEM (HAADF-STEM) images were acquired at 200 kV with the probe Cs-corrector configuration. X-ray photoelectron spectroscopy (XPS) analyses were conducted on an ESCALAB 250 Xi X-ray photoelectron spectrometer using Al Kα radiation. Specific surface area measurements were conducted on a QuadraSorb SI automated surface area and pore size analyzer (Quantachrome Instruments). The Pd content of each sample was determined by inductively coupled plasma atomic emission spectroscopy (ICP-AES, Thermo Scientific).

2.9 Catalyst performance measurements

The catalytic properties of the prepared catalysts toward the partial hydrogenation of acetylene were evaluated under atmospheric pressure in a continuous flow fixed-bed quartz tubular reactor. In a typical process, 100 mg of the catalyst was mixed with quartz sand and placed in the reactor. The reactant gas mixture (0.65 vol% acetylene, 5 vol% hydrogen, and 50.0 vol% ethylene balanced with argon) was passed through the reactor at a flow rate of 40 mL·min^{-1}. The composition of the outlet gas was recorded by gas chromatography. Conversion and selectivity were calculated according to a previous report [22]. The turnover frequency (TOF) of the catalyst was determined as the rate of acetylene consumed per number of surface-exposed Pd sites.

3 Results and discussion

To prepare the atomically dispersed 0.005% Pd/Ni(OH)$_2$ catalyst, the large specific surface area Ni(OH)$_2$ support (231.5 m^2·g^{-1}, Fig. S1 in the Electronic Supplementary Material (ESM)) was first fabricated. Sufficient impregnation of the appropriate amount of the Pd precursor into a well-dispersed Ni(OH)$_2$ suspension and subsequent reduction afforded the 0.005% Pd/Ni(OH)$_2$

catalyst. A 0.8% Pd/Ni(OH)$_2$ catalyst was also fabricated as a reference using a similar preparative method. Figure S2 in the ESM displays the XRD patterns of the as-prepared catalysts. The profiles of 0.8% and 0.005% Pd/Ni(OH)$_2$ catalysts were well matched to that of the Ni(OH)$_2$ support and could be assigned to the characteristic peaks of Ni(OH)$_2$ (JCPDS 38-0715) [23].

The prepared catalysts were subsequently evaluated for their abilities to catalyze the selective hydrogenation of acetylene to ethylene. As displayed in Fig. S3 in the ESM, the Ni(OH)$_2$ support exhibits negligible catalytic acetylene conversion over the temperature range employed, while the results displayed in Fig. S4 in the ESM show that the 0.8% Pd/Ni(OH)$_2$ material is capable of fully catalyzing the conversion of acetylene in the 35–60 ℃ temperature range, but the corresponding selectivity for ethylene is very poor and below 20%.

Interestingly, as shown in Fig. 2(a), the TOF for acetylene conversion over the 0.005% Pd/Ni(OH)$_2$ catalyst is 0.164 s^{-1} at 75 ℃, which is twice that of the 0.8% Pd/Ni(OH)$_2$ catalyst (0.081 s^{-1}). Full conversion of acetylene over the 0.005% Pd/Ni(OH)$_2$ catalyst is obtained at 120 ℃, as displayed in Fig. 2(b). Strikingly, the Pd/Ni(OH)$_2$ catalyst with the ultra-low 0.005% palladium loading exhibits excellent ethylene selectivity compared to that of its higher palladium-loaded counterpart, as shown in Fig. 2(c). In the 80–105 ℃ temperature region, ethylene selectivity is essentially maintained, at around 80%, using the 0.005% Pd/Ni(OH)$_2$ catalyst. When the acetylene content was near to full conversion, the corresponding ethylene selectivity decreased, which is a phenomenon commonly observed in acetylene hydrogenation processes and has been ascribed to the different adsorption strengths of acetylene and ethylene at the active Pd sites [13]. Acetylene is more thermodynamically favored over ethylene for Pd adsorption and activation. However, as the acetylene approaches complete consumption, ethylene can competitively adsorb to the active Pd sites, leading to a decrease in ethylene selectivity. Time-on-stream stability testing at 105 ℃ over the 0.005% Pd/Ni(OH)$_2$ catalyst (Fig. 2(d)) reveals that both acetylene conversion and ethylene selectivity are well maintained at around 80% over the 12 h testing duration, indicating that the 0.005% Pd/Ni(OH)$_2$ catalyst has excellent stability.

To explore the underlying reasons for the excellent

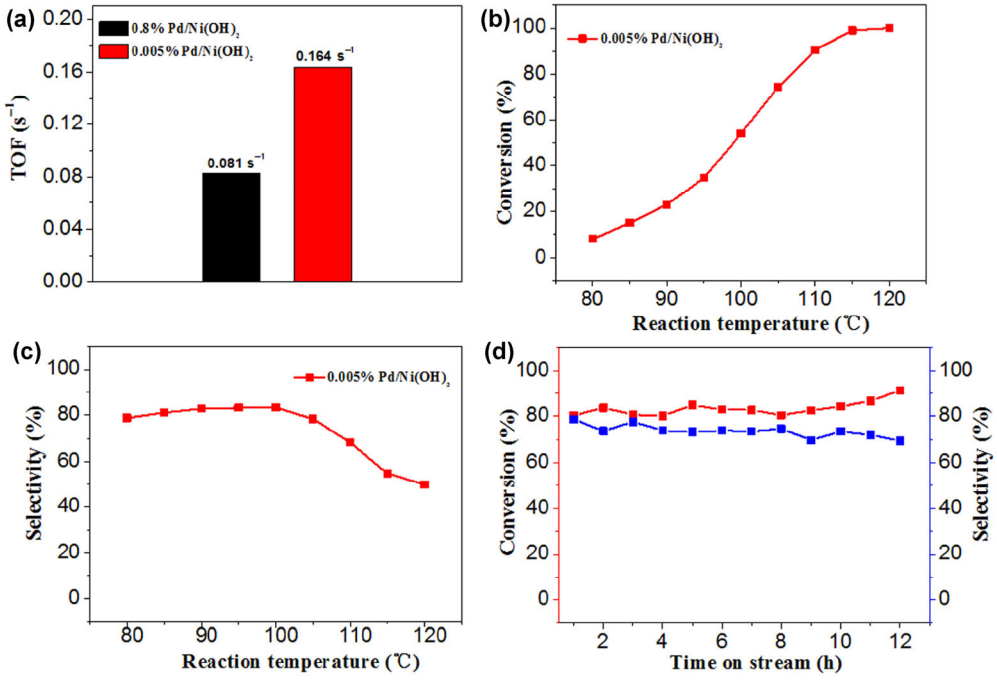

Figure 2 (a) TOF values for the 0.8% and 0.005% Pd/Ni(OH)$_2$ catalysts at 75 ℃. (b) Acetylene conversion and (c) ethylene selectivities as functions of temperature for acetylene conversion over the 0.005% Pd/Ni(OH)$_2$ catalyst. (d) Time-on-stream stability testing over the 0.005% Pd/Ni(OH)$_2$ catalyst at 105 ℃.

catalytic properties exhibited by the 0.005% Pd/Ni(OH)$_2$ catalyst, detailed characterization experiments were performed.

The surface structures of the prepared catalysts were characterized by XPS. The Ni 2p XPS spectra (Fig. S5(a) in the ESM) reveal binding-energy peaks centered at about 855.9 eV that correspond to Ni^{2+} in Ni(OH)$_2$ [24, 25]. The Pd 3d XPS spectrum in Fig. S5(b) in the ESM exhibits binding-energy peaks centered at about 335.2 and 340.2 eV reveals for the 0.8% Pd/Ni(OH)$_2$ catalyst; these are ascribed to the Pd $3d_{5/2}$ and Pd $3d_{3/2}$ peaks of metallic palladium [26–28]. However, no obvious Pd 3d peak can be resolved for the 0.005% Pd/Ni(OH)$_2$ catalyst, due to its ultra-low Pd content. For the same reason, this catalyst was unable to be characterized by extended X-ray absorption fine structure (EXAFS) analysis.

It is well known that the hydrogenation of acetylene is a structure-sensitive reaction, and the active-site particle sizes greatly influence the corresponding catalytic performance [29]. Figures 3(a) and 3(b) depict the high-resolution TEM (HRTEM) and HAADF-STEM images of the 0.8% Pd/Ni(OH)$_2$ catalyst; the Pd nanoparticles are observed to be evenly dispersed over the Ni(OH)$_2$ nanosheets, with an average particle size of 1.7 nm, as revealed statistically in Fig. S6 in the ESM. Figure 3(c) depicts the HAADF-STEM image of the 0.005% Pd/Ni(OH)$_2$ catalyst. Due to the highly dispersed ultra-low palladium loading on the Ni(OH)$_2$ support, no Pd nanoparticles are observed. Consequently, we characterized the 0.005% Pd/Ni(OH)$_2$ catalyst using the powerful aberration-corrected HAADF-STEM technique that is commonly used for the characterization of atomically dispersed materials.

Detailed examinations of different regions of the catalyst, as shown in Fig. 3(d) and Fig. S7 in the ESM, failed to reveal any Pd particle, further confirming the atomically dispersed nature of the Pd sites in the 0.005% Pd/Ni(OH)$_2$ catalyst.

The excellent activity and selectivity observed for the 0.005% Pd/Ni(OH)$_2$ catalyst may be the result of the atomically dispersed nature of its Pd sites, compared to the reference Pd nanoparticles in the 0.8% Pd/Ni(OH)$_2$ catalyst. Previous research demonstrated that decoupling the Pd ensembles and increasing the number of isolated Pd atoms effectively restricts the formation of unfavorable ethylidene intermediates, carbide, and active subsurface hydrogen species that are intimately associated with the total hydrogenation of acetylene [11, 30, 31]. Furthermore, isolated-palladium-atom catalysts were found to exhibit facile hydrogen and alkyne activation abilities, which facilitate alkyne adsorption and the subsequent desorption of ethylene from the catalyst surface [12, 32], greatly favoring the selective hydrogenation of acetylene to ethylene. Our results are consistent with these reported findings.

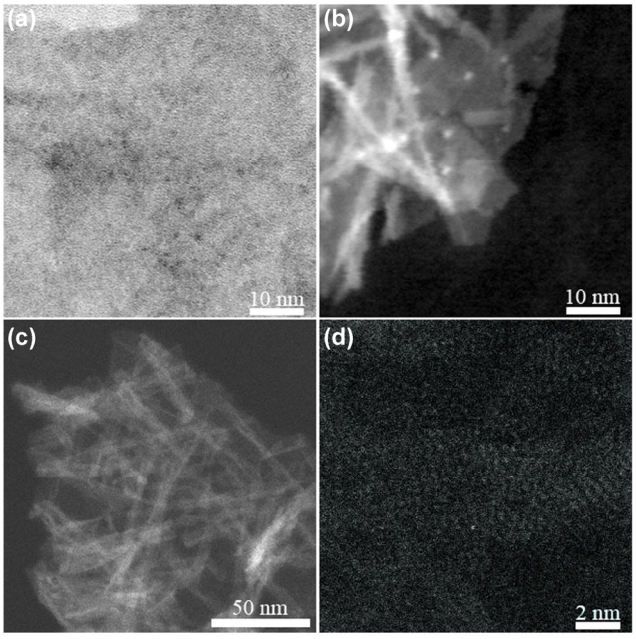

Figure 3 (a) HRTEM and (b) HAADF-STEM images of the 0.8% Pd/Ni(OH)$_2$ catalyst. (c) HAADF-STEM and (d) aberration-corrected HAADF-STEM images of the 0.005% Pd/Ni(OH)$_2$ catalyst.

In addition to the nature of the active component, the support itself has been demonstrated in many studies to affect catalytic performance [33, 34]. Consequently, we examined a series of supports to check the general applicability of this ultra-low-loaded palladium catalyst. We first prepared an atomically dispersed 0.005% Pd/NiO catalyst to explore the effect of the support in this reaction. Catalytic studies (Fig. S8 in the ESM) reveal that the 0.005% Pd/NiO catalyst exhibits a remarkable decrease in acetylene conversion when compared with the 0.005% Pd/Ni(OH)$_2$ catalyst, while maintaining a similar catalytic selectivity for the formation of ethylene. The most obvious difference between the 0.005% Pd/Ni(OH)$_2$ and 0.005% Pd/NiO

catalyst is the abundance of hydroxyl groups on the surface of the $Ni(OH)_2$ support; OH groups have been found to greatly influence the catalytic activities of some reaction systems [35, 36]. We speculated that the OH groups of the support may also play key roles in determining acetylene conversion activity of our catalyst. To examine this hypothesis, we further prepared robust mesoporous SiO_2 supports, as displayed in Figs. S9 and S10 in the ESM. By varying the calcination temperature, the surface Si–OH content of the mesoporous SiO_2 support is readily tuned. In addition, the Si–OH structures are easily restored by deliberately re-dispersing the mesoporous SiO_2 support in water; this offers the opportunity to systematically explore the effect of OH groups in the selective hydrogenation of acetylene.

Figure 4(a) shows the FT-IR spectra of the mesoporous SiO_2 supports and a series of 0.005% Pd/SiO_2-*T* catalysts (*T* refers to calcination temperature, see the ESM for details). The FT-IR bands at around 1,080 and 800 cm^{-1} are ascribed to the asymmetric and symmetric vibrations of the mesoporous SiO_2 framework [37]. The band at 960 cm^{-1} corresponds to Si–OH stretching vibrations and can serves as an indicator of surface Si–OH content [37, 38]. After calcination at 750 ℃, the surface Si–OH content of the 0.005% Pd/SiO_2-750 catalyst was found to have decreased significantly when compared with those of the mesoporous SiO_2 support and the 0.005% Pd/SiO_2-300 catalyst. When the 0.005% Pd/SiO_2-750 material was re-dispersed in water and then dried, the 0.005% Pd/SiO_2-750RD catalyst obtained in this manner generally exhibited restored surface Si–OH structures in its FT-IR spectrum (Fig. 4(a)). The corresponding catalysis results (Fig. 4(b)) reveal that acetylene conversion over the 0.005% Pd/SiO_2-750 catalyst was sharply lower than that of the reference 0.005% Pd/SiO_2-300 catalyst, consistent with the differences in their Si–OH contents. After restoration of the Si–OH structures, the 0.005% Pd/SiO_2-750RD catalyst exhibited almost the same acetylene conversion as a function of temperature as the 0.005% Pd/SiO_2-300 catalyst, unambiguously revealing the key roles of the OH groups in determining acetylene conversion activity. It should be noted that the corresponding ethylene selectivity over the 0.005% Pd/SiO_2-300, 0.005% Pd/SiO_2-750, and 0.005% Pd/SiO_2-750RD catalysts remained similar at the same acetylene conversions, as indicated in Fig. S11 in the ESM. These results reveal the strong OH-dependent-activity behavior of the atomically dispersed Pd catalysts. Recent DFT calculations and experimental results demonstrated that the activation of hydrogen by atomically dispersed Pd catalysts commonly involves a heterolytic dissociation process that generates negatively charged $Pd–H^{\delta-}$. The positively charged H-atom counterpart tends to bond with the surrounding chemical groups of the support [12, 14]. In the current case, we speculate that the resulting positively charged H atom may be also bond to the OH groups of the support. When the numbers of these OH groups are reduced by calcination, the activation of hydrogen was unavoidably hampered, resulting in an accompanying decrease in catalytic activity.

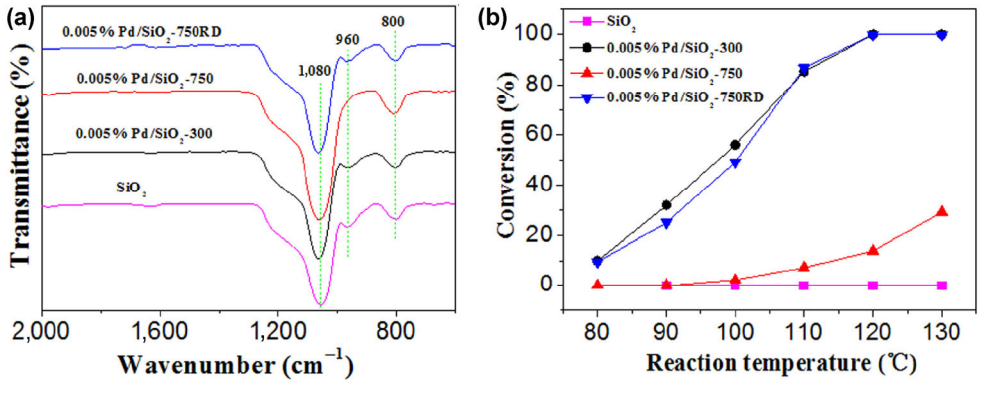

Figure 4 (a) FT-IR spectra and (b) corresponding acetylene conversions for the SiO_2 support, 0.005% Pd/SiO_2-300, 0.005% Pd/SiO_2-750, and 0.005% Pd/SiO_2-750RD catalysts.

4 Conclusions

In summary, we successfully fabricated a Pd/Ni(OH)$_2$ catalyst loaded with ultra-low levels (0.005%) of atomically dispersed palladium that exhibits excellent catalytic activity and selectivity toward the hydrogenation of acetylene to ethylene. Detailed experimental results further reveal that the atomically dispersed nature of palladium and the hydroxyl groups of the support are of great importance in determining the performance of the catalyst. The excellent catalytic properties and cost-effective preparation endow the 0.005% Pd/Ni(OH)$_2$ catalyst with great potential for use in practical applications. We believe that this new kind of catalyst may also be employable in a variety of reactions such homogeneous and heterogeneous catalytic hydrogenations, opening up opportunities for the use of trace-loaded noble metals as cost-effective catalysts.

Acknowledgements

This work was supported by the National Key Research and Development Program of China (No. 2016YFA0202801) and the National Natural Science Foundation of China (Nos. 21521091, 21573119, 21590792, 21390393, U1463202, and 21473199), Beijing Municipal Science & Tech-nology Commission and Chinese Academy of Sciences.

Electronic Supplementary Material: Supplementary material (TEM imaging, XRD and XPS spectroscopy measurements, and supplementary catalytic evaluation of the prepared catalysts) is available in the online version of this article at https://doi.org/10.1007/s12274-017-1701-5.

References

[1] Teschner, D.; Borsodi, J.; Wootsch, A.; Révay, Z.; Hävecker, M.; Knop-Gericke, A.; Jackson, S. D.; Schlögl, R. The roles of subsurface carbon and hydrogen in palladium-catalyzed alkyne hydrogenation. *Science* **2008**, *320*, 86–89.

[2] Huang, W.; McCormick, J. R.; Lobo, R. F.; Chen, J. G. Selective hydrogenation of acetylene in the presence of ethylene on zeolite-supported bimetallic catalysts. *J. Catal.* **2007**, *246*, 40–51.

[3] Borodziński, A.; Bond, G. C. Selective hydrogenation of ethyne in ethene-rich streams on palladium catalysts, part 2: Steady-state kinetics and effects of palladium particle size, carbon monoxide, and promoters. *Catal. Rev.* **2008**, *50*, 379–469.

[4] Armbrüster, M.; Kovnir, K.; Friedrich, M.; Teschner, D.; Wowsnick, G.; Hahne, M.; Gille, P.; Szentmiklósi, L.; Feuerbacher, M.; Heggen, M. et al. $Al_{13}Fe_4$ as a low-cost alternative for palladium in heterogeneous hydrogenation. *Nat. Mater.* **2012**, *11*, 690–693.

[5] Schütte, K.; Doddi, A.; Kroll, C.; Meyer, H.; Wiktor, C.; Gemel, C.; van Tendeloo, G.; Fischer, R. A.; Janiak, C. Colloidal nickel/gallium nanoalloys obtained from organometallic precursors in conventional organic solvents and in ionic liquids: Noble-metal-free alkyne semihydrogenation catalysts. *Nanoscale* **2014**, *6*, 5532–5544.

[6] Studt, F.; Abild-Pedersen, F.; Bligaard, T.; Sørensen, R. Z.; Christensen, C. H.; Nørskov, J. K. Identification of non-precious metal alloy catalysts for selective hydrogenation of acetylene. *Science* **2008**, *320*, 1320–1322.

[7] Liu, Y. X.; Liu, X. W.; Feng, Q. C.; He, D. S.; Zhang, L. B.; Lian, C.; Shen, R. A.; Zhao, G. F.; Ji, Y. J.; Wang, D. S. et al. Intermetallic Ni_xM_y (M = Ga and Sn) nanocrystals: A non-precious metal catalyst for semi-hydrogenation of alkynes. *Adv. Mater.* **2016**, *28*, 4747–4754.

[8] Armbrüster, M.; Kovnir, K.; Behrens, M.; Teschner, D.; Grin, Y.; Schlögl, R. Pd−Ga intermetallic compounds as highly selective semihydrogenation catalysts. *J. Am. Chem. Soc.* **2010**, *132*, 14745–14747.

[9] Niu, W. X.; Gao, Y. J.; Zhang, W. Q.; Yan, N.; Lu, X. M. Pd–Pb alloy nanocrystals with tailored composition for semihydrogenation: Taking advantage of catalyst poisoning. *Angew. Chem., Int. Ed.* **2015**, *54*, 8271–8274.

[10] Studt, F.; Abild-Pedersen, F.; Bligaard, T.; Sørensen, R. Z.; Christensen, C. H.; Nørskov, J. K. On the role of surface modifications of palladium catalysts in the selective hydrogenation of acetylene. *Angew. Chem., Int. Ed.* **2008**, *47*, 9299–9302.

[11] Kyriakou, G.; Boucher, M. B.; Jewell, A. D.; Lewis, E. A.; Lawton, T. J.; Baber, A. E.; Tierney, H. L.; Flytzani-Stephanopoulos, M.; Sykes, E. C. H. Isolated metal atom geometries as a strategy for selective heterogeneous hydrogenations. *Science* **2012**, *335*, 1209–1212.

[12] Vilé, G.; Albani, D.; Nachtegaal, M.; Chen, Z. P.; Dontsova, D.; Antonietti, M.; López, N.; Pérez-Ramírez, J. A stable single-site palladium catalyst for hydrogenations. *Angew. Chem., Int. Ed.* **2015**, *54*, 11265–11269.

[13] McCue, A. J.; Anderson, J. A. Recent advances in selective acetylene hydrogenation using palladium containing catalysts. *Front. Chem. Sci. Eng.* **2015**, *9*, 142–153.

[14] Liu, P. X.; Zhao, Y.; Qin, R. X.; Mo, S. G.; Chen, G. X.; Gu, L.; Chevrier, D. M.; Zhang, P.; Guo, Q.; Zang, D. D. et al. Photochemical route for synthesizing atomically dispersed palladium catalysts. *Science* **2016**, *352*, 797–800.

[15] Yang, X.-F.; Wang, A. Q.; Qiao, B. T.; Li, J.; Liu, J. Y.; Zhang, T. Single-atom catalysts: A new frontier in heterogeneous catalysis. *Acc. Chem. Res.* **2013**, *46*, 1740–1748.

[16] Qiao, B. T.; Wang, A. Q.; Yang, X. F.; Allard, L. F.; Jiang, Z.; Cui, Y. T.; Liu, J. Y.; Li, J.; Zhang, T. Single-atom catalysis of CO oxidation using Pt_1/FeO_x. *Nat. Chem.* **2011**, *3*, 634–641.

[17] Gao, D. W.; Zhang, X.; Yang, Y.; Dai, X. P.; Sun, H.; Qin, Y. C.; Duan, A. J. Supported single Au(III) ion catalysts for high performance in the reactions of 1,3-dicarbonyls with alcohols. *Nano Res.* **2016**, *9*, 985–995.

[18] Long, B.; Tang, Y.; Li, J. New mechanistic pathways for CO oxidation catalyzed by single-atom catalysts: Supported and doped Au_1/ThO_2. *Nano Res.* **2016**, *9*, 3868–3880.

[19] Liu, J. Y. Catalysis by supported single metal atoms. *ACS Catal.* **2017**, *7*, 34–59.

[20] Du, H. M.; Jiao, L. F.; Cao, K. Z.; Wang, Y. J.; Yuan, H. T. Polyol-mediated synthesis of mesoporous α-$Ni(OH)_2$ with enhanced supercapacitance. *ACS Appl. Mater. Interfaces* **2013**, *5*, 6643–6648.

[21] Tüysüz, H.; Hwang, Y. J.; Khan, S. B.; Asiri, A. M.; Yang, P. D. Mesoporous Co_3O_4 as an electrocatalyst for water oxidation. *Nano Res.* **2013**, *6*, 47–54.

[22] Yang, J.; Zhang, F. J.; Lu, H. Y.; Hong, X.; Jiang, H. L.; Wu, Y.; Li, Y. D. Hollow Zn/Co ZIF particles derived from core–shell ZIF-67@ZIF-8 as selective catalyst for the semi-hydrogenation of acetylene. *Angew. Chem., Int. Ed.* **2015**, *54*, 10889–10893.

[23] Gao, M. R.; Sheng, W. C.; Zhuang, Z. B.; Fang, Q. R.; Gu, S.; Jiang, J.; Yan, Y. S. Efficient water oxidation using nanostructured α-nickel-hydroxide as an electrocatalyst. *J. Am. Chem. Soc.* **2014**, *136*, 7077–7084.

[24] Yan, J.; Fan, Z. J.; Sun, W.; Ning, G. Q.; Wei, T.; Zhang, Q.; Zhang, R. F.; Zhi, L. J.; Wei, F. Advanced asymmetric supercapacitors based on $Ni(OH)_2$/graphene and porous graphene electrodes with high energy density. *Adv. Funct. Mater.* **2012**, *22*, 2632–2641.

[25] Wu, J.; Ren, Z. Y.; Du, S. C.; Kong, L. J.; Liu, B. W.; Xi, W.; Zhu, J. Q.; Fu, H. G. A highly active oxygen evolution electrocatalyst: Ultrathin CoNi double hydroxide/CoO nanosheets synthesized via interface-directed assembly. *Nano Res.* **2016**, *9*, 713–725.

[26] Li, R. S.; Mao, H.; Zhang, J. J.; Huang, T.; Yu, A. S. Rapid synthesis of porous Pd and PdNi catalysts using hydrogen bubble dynamic template and their enhanced catalytic performance for methanol electrooxidation. *J. Power Sources* **2013**, *241*, 660–667.

[27] Demirci, U. B. Theoretical means for searching bimetallic alloys as anode electrocatalysts for direct liquid-feed fuel cells. *J. Power Sources* **2007**, *173*, 11–18.

[28] Slanac, D. A.; Hardin, W. G.; Johnston, K. P.; Stevenson, K. J. Atomic ensemble and electronic effects in Ag-rich AgPd nanoalloy catalysts for oxygen reduction in alkaline media. *J. Am. Chem. Soc.* **2012**, *134*, 9812–9819.

[29] Jin, Q.; He, Y. F.; Miao, M. Y.; Guan, C. Y.; Du, Y. Y.; Feng, J. T.; Li, D. Q. Highly selective and stable PdNi catalyst derived from layered double hydroxides for partial hydrogenation of acetylene. *Appl. Catal. A* **2015**, *500*, 3–11.

[30] Armbrüster, M.; Wowsnick, G.; Friedrich, M.; Heggen, M.; Cardoso-Gil, R. Synthesis and catalytic properties of nanoparticulate intermetallic Ga–Pd compounds. *J. Am. Chem. Soc.* **2011**, *133*, 9112–9118.

[31] Boudart, M.; Hwang, H. S. Solubility of hydrogen in small particles of palladium. *J. Catal.* **1975**, *39*, 44–52.

[32] Zhou, H. R.; Yang, X. F.; Li, L.; Liu, X. Y.; Huang, Y. Q.; Pan, X. L.; Wang, A. Q.; Li, J.; Zhang, T. PdZn intermetallic nanostructure with Pd–Zn–Pd ensembles for highly active and chemoselective semi-hydrogenation of acetylene. *ACS Catal.* **2016**, *6*, 1054–1061.

[33] Ishida, T.; Kinoshita, N.; Okatsu, H.; Akita, T.; Takei, T.; Haruta, M. Influence of the support and the size of gold clusters on catalytic activity for glucose oxidation. *Angew. Chem., Int. Ed.* **2008**, *47*, 9265–9268.

[34] Yoon, B.; Häkkinen, H.; Landman, U.; Wörz, A. S.; Antonietti, J.-M.; Abbet, S.; Judai, K.; Heiz, U. Charging effects on bonding and catalyzed oxidation of CO on Au_8 clusters on MgO. *Science* **2005**, *307*, 403–407.

[35] Qian, K.; Zhang, W. H.; Sun, H. X.; Fang, J.; He, B.; Ma, Y. S.; Jiang, Z. Q.; Wei, S. Q.; Yang, J. L.; Huang, W. X. Hydroxyls-induced oxygen activation on "inert" Au nanoparticles for low-temperature CO oxidation. *J. Catal.* **2011**, *277*, 95–103.

[36] Zhai, Y. P.; Pierre, D.; Si, R.; Deng, W. L.; Ferrin, P.; Nilekar, A. U.; Peng, G. W.; Herron, J. A.; Bell, D. C.; Saltsburg, H. et al. Alkali-stabilized Pt-OH_x species catalyze low-temperature water-gas shift reactions. *Science* **2010**, *329*, 1633–1636.

[37] Liu, Z. C.; Zhou, J.; Cao, K.; Yang, W. M.; Gao, H. X.; Wang, Y. D.; Li, H. X. Highly dispersed nickel loaded on mesoporous silica: One-spot synthesis strategy and high performance as catalysts for methane reforming with carbon dioxide. *Appl. Catal. B* **2012**, *125*, 324–330.

[38] Tsoncheva, T.; Ivanova, L.; Rosenholm, J.; Linden, M. Cobalt oxide species supported on SBA-15, KIT-5 and KIT-6 mesoporous silicas for ethyl acetate total oxidation. *Appl. Catal. B* **2009**, *89*, 365–374.